Preprint, 11th IFAC Symposium on Dynamics and Control of Process Systems, including Biosystems
June 6-8, 2016. NTNU, Trondheim, Norway

Control of a Solar Furnace using MPC with Integral Action

Bertinho A. Costa * **João M. Lemos** ** **Emmanuel Guillot** ***

* *INESC-ID/IST, University of Lisbon, Rua Alves Redol, 9 1000-029, Portugal (e-mail: bac@inesc-id.pt).*
** *INESC-ID/IST, University of Lisbon, Rua Alves Redol, 9 1000-029, Portugal (e-mail: jlml@inesc-id.pt).*
*** *CNRS-PROMES, 7 rue du Four Solaire, 66120 Font Romeu Odeillo, France (e-mail: emmanuel.guillot@promes.cnrs.fr).*

Abstract:
Solar furnaces are devices employed in high temperature material stress tests that use concentrated solar energy. This process has a nonlinear dynamics caused by a fourth power temperature term and by the nonlinear behavior of the shutter. Sun power variability due to weather conditions may affect the operation of a solar furnace if it is not compensated by adjusting the shutter aperture. The contribution of this paper is to explore and to evaluate the application of model predictive control with integral action to a nonlinear process. Off-line identification is employed to characterize the temperature dynamics. This methodology avoids the use of online adaptation mechanisms that may cause stability problems during temperature stress tests that may melt the material sample. The aim is to design a controller with a good performance, able to track the temperature cycling profile without overshooting to avoid melting the material sample. Active cooling is also explored to improve the temperature tracking during the decrease of the temperature profile. Experimental results obtained from the closed loop control of the plant are presented.

Keywords: Solar Furnace, Non-linear Dynamics, Off-line Identification, Incremental Model Predictive Control.

Fig. 1. PROMES laboratory at Odeillo, southern France, with the 1MW parabolic mirror. Smaller size solar furnaces are located at the southern part of the building.

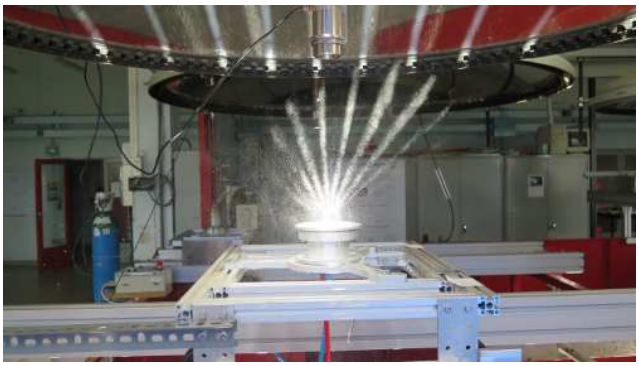

Fig. 2. Visualization of the focus of the 900W solar furnace at PROMES with water spray.

1. INTRODUCTION

The PROMES Solar Energy Laboratory at Odeillo, southern France (fig. 1) and the Plataforma Solar de Almeria (southern Spain) Berenguel et al. (1999) are two sites that use concentrated solar energy to develop solar energy applications, such as material stress tests.

Solar furnaces are devices that concentrate solar energy, that may be used to characterize the behaviour of materials using temperature (or power) cycling stress tests. A solar furnace comprises an heliostat that tracks the sun and guides the solar energy to a parabolic mirror that concentrates energy on a focus. The energy applied on the material sample is adjusted by commanding the shutter aperture. Figure 2 shows the focus of the 900W solar furnace at PROMES using a water spray. The size of the light strips depend on the shutter aperture.

The temperature dynamics of a sample has a nonlinear behavior that depends on its size, the material properties,

⋆ This work was developed under the european project SFERA2 and the program UID/CEC/50021/2013.

the power losses by radiation and by convection, and the energy absorption.

Uncertainty on the material thermodynamic properties, the balance of energy, and the aperture of the shutter that has a nonlinear effect on the amount of incident energy on the sample affect process dynamics. Solar power fluctuations induced by the presence of clouds, if not compensated, affect the operation of the solar furnaces and the results of temperature stress experiments.

An enhanced temperature control architecture was proposed in Costa and Lemos (2009) where the aim was to explore a cascade control architecture with two loops to decouple the shutter nonlinearity from the temperature dynamics. In Costa and Lemos (2012) a predictive adaptive controller was used in parallel with a PI controller to control the temperature of the sample. The aim was to use the adaptive controller to improve the performance in situations where the PI controller was not well tuned. However, in this approach the use of online adaptation may cause stability problems.

An alternative approach based on a PI controller with exact linearization proposed in Costa and Lemos (2014a) was tested experimentally showing good results Costa and Lemos (2016). In Costa and Lemos (2014b) optimal control is evaluated to control a solar furnace. Comparing the results obtained with the PI controller with exact linearization and with the MPC with integral action, it can be concluded that the reference tracking is similar but the MPC provides a smoother control action.

In this paper the proposed control law is obtained by following similar steps as in other predictive controllers, such as, the GPC Clarke et al. (1987) but with the linear model being obtained by on-line linearization around the reference. Process output predictors are employed to minimize a cost function that weights the tracking error and the control increments (integral action). In this case the process has a nonlinear dynamics. A Taylor expansion is used to approximate the process dynamics around the reference. This causes the output predictors to have parameters that depend on future values of the reference.

Two adjustable parameters, the number of predictors and the weight on the control action, are used to select the controller gains. In this framework off-line model identification is employed to characterize the temperature dynamics. The identified model includes the contribution of the losses by convection and by radiation.

From the results obtained it is concluded that the weight on the control action is the most important parameter that affect the performance of the closed-loop process.

2. SOLAR FURNACE MODEL

The solar furnace model comprises two dynamic models: a dynamic model that describes the interactions between the concentrated solar energy and the temperature of the sample, and the model that describes the behaviour of the shutter. These models are presented hereafter.

Table 1. Thermal model parameters

Parameter : **Description**
$\rho\ [kgm^{-3}]$: Density of the material
$C_p\ [Jkg^{-1}K^{-1}]$: Material Specific Heat
$m\ [kg]$: Mass of the sample
ϵ : Emissivity of the material
$\sigma\ [Wm^{-2}K^{-4}]$: Stefan-Boltzmann const.
$A_{sr}\ [m^2]$: Sample's loss radiation area
$A_{sc}\ [m^2]$: Sample's convection area
$A_{si}\ [m^2]$: Sample's incident area
$L_c\ [m]$: Characteristic length
$h_{conv}\ [Wm^{-2}K^{-1}]$: Convection factor
α_s : Sample's solar absorption factor
g_f : Furnace gain
$G_s\ [W/m^2]$: Max. Solar Flux

2.1 Shutter model

The shutter operates in closed loop using a servo mechanism. The shutter has a dynamics that is much faster than the thermal model subsystem, and thus only the static function of the shutter is considered,

$$s_{fs}(u_s(t)) = 1 - \frac{\cos(\theta_0 + u_s(t)(90^\circ - \theta_0)/100)}{\cos(\theta_0)}\,, \qquad (1)$$

with the shutter command being limited to, $0 \leq u_s(t) \leq 100$ and $\theta_0 = 25^\circ$. The controller of the shutter is able to move the blades to the target angle in less than $0.2s$.

2.2 Temperature model of the sample

An energy balance is used to model the temperature of the sample, such as the one made in Berenguel et al. (1999). The samples can have different shapes and sizes, but a circular shape with a diameter of $2cm$ and a height of $2mm$ can be considered a typical sample size. The temperature of the sample, $T_s(t)$ [K] is described (approximated) by

$$\frac{dT_s(t)}{dt} = -\alpha_1[T_s^4(t) - T_b^4(t)] - \alpha_2[T_s(t) - T_e(t)] \qquad (2)$$
$$+\alpha_3 G_s(t) s_{fs}(u_s(t))\,.$$

T_b [K] represents the temperature of the "environment" that contributes to losses by radiation and T_e represents the temperature of the surrounding air that contributes to losses by convection. The factors α_1 , α_2 and α_3 represent the process parameters, being defined by

$$\alpha_1 = \frac{\epsilon(T_s)\sigma A_{sr}}{C_p(T_s)m};\ \alpha_2 = \frac{h_{conv}(T_s, T_e)A_{sc}}{C_p(T_s)m};\ \alpha_3 = \frac{\alpha_s A_{si} g_f}{C_p(T_s)m}\,. \qquad (3)$$

These parameters are estimated using data collected from the process as shown in fig. 3, where the shutter was commanded manually do change the temperature of a stainless steel sample. In order to perform the process identification $G_s(.)$ (available sun power) is also recorded.

The parameters in 3 are described in Table 1.

3. OFF-LINE IDENTIFICATION OF THE TEMPERATURE MODEL

From the literature it can be concluded that parameters α_1 , α_2 and α_3 depend on temperature on a small degree for a large set of materials. Thus they can be assumed to

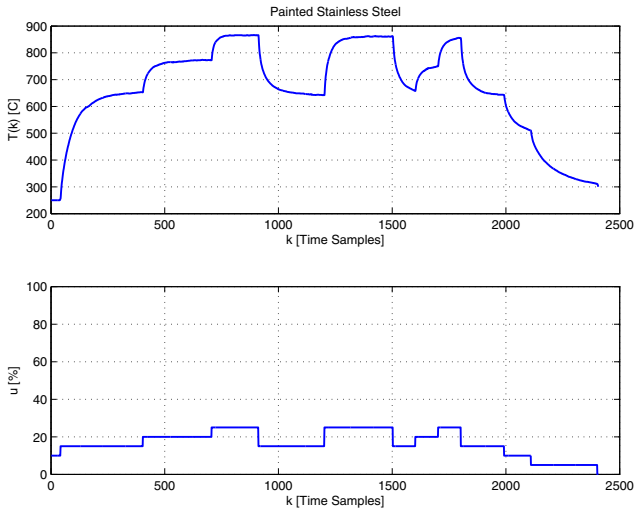

Fig. 3. Data collected from the solar furnace by manually adjusting the shutter. The material sample temperature is shown at the top and the manipulated variable is shown at the bottom. The solar power was almost constant during the experiment ($950W/m^2$).

be constant. This assumption can be validated during the identification process.

In order to estimate the parameters, sample data is used. The continuous time model is filtered by a first order filter followed by a conversion to a discrete time model. Hence, the following signals are defined, $\zeta_1(t) = [T_s^4(t) - T_e^4(t)]$, $\zeta_2(t) = [T_s(t) - T_e(t)]$ and $\zeta_3(t) = u_r(t) = G_s(t)s_{fs}(u_s(t))$, and a stable low-pass filter $O(s) = a/(s+a)$ with unitary static gain is applied to (2), yielding

$$\frac{as}{(s+a)}T_s(s) = -\alpha_1\frac{a\zeta_1(s)}{(s+a)} - \alpha_2\frac{a\zeta_2(s)}{(s+a)} + \alpha_3\frac{a\zeta_3(s)}{(s+a)}\,. \quad (4)$$

The value of parameter $a > 0$ is selected based on the level of noise present on $T_s(.)$ and on the dynamics of the process. The general rule is to select the filter to be much faster than the temperature dynamics. It follows that (4) admits the continuous time representation,

$$\zeta_{f0}(t) = -\alpha_1\zeta_{f1}(t) - \alpha_2\zeta_{f2}(t) + \alpha_3\zeta_{f3}(t) \quad (5)$$

with

$$\zeta_{f0}(t) = a(T_s(t) - T_{sf}(t)) \quad (6)$$

$$\frac{dT_{sf}(t)}{dt} = -aT_{sf}(t) + aT_s(t) \quad (7)$$

$$\frac{d\zeta_{f1}(t)}{dt} = -a\zeta_{f1}(t) + a\zeta_1(t) \quad (8)$$

$$\frac{d\zeta_{f2}(t)}{dt} = -a\zeta_{f2}(t) + a\zeta_2(t) \quad (9)$$

$$\frac{d\zeta_{f3}(t)}{dt} = -a\zeta_{f3}(t) + a\zeta_3(t)\,. \quad (10)$$

In order to solve these dynamic equations in discrete time, the first order hold (FOH) method is applied using the sampling time $h = 0.5s$. The estimation of parameters α_1 , α_2 and α_3 are computed with the Least Mean Square (LMS) method using the discrete time signals $\zeta_{f0}[t]$, $\zeta_{f1}[t]$, $\zeta_{f2}[t]$, $\zeta_{f3}[t]$.

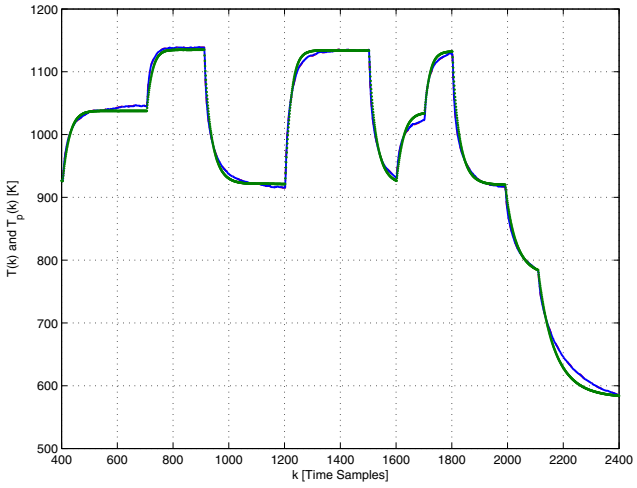

Fig. 4. Off-line model identification. Sample temperature $T_s(t)$ (blue colour) and the one-step ahead prediction are very similar. The model output with the initial state set to $T_s[400]$ is shown in green colour. In both cases model output gives a good approximation of the process dynamics.

Considering eq. (5) and the data at each time sample, it follows that

$$\begin{bmatrix} y[t] \\ y[t-h] \\ \dots \\ y[t-nh] \end{bmatrix} = \begin{bmatrix} \zeta_{f1}[t] & \zeta_{f2}[t] & \zeta_{f3}[t] \\ \zeta_{f1}[t-h] & \zeta_{f2}[t-h] & \zeta_{f3}[t-h] \\ \dots & \dots & \dots \\ \zeta_{f1}[t-nh] & \zeta_{f2}[t-nh] & \zeta_{f3}[t-nh] \end{bmatrix} \begin{bmatrix} \alpha_1 \\ \alpha_2 \\ \alpha_3 \end{bmatrix}, \quad (11)$$

that can be represented as $Y = \Phi\alpha$. The parameters are obtained from

$$\alpha = (\Phi^T\Phi)^{-1}\Phi Y \quad (12)$$

where the matrix $\Phi^T\Phi$ must have inverse. The validity of this assumption depends on the spectrum content of the control signal that must be "rich". In the present work, the shutter is operated by steps to evaluate the time response of the (material sample) temperature. Note that, in the present problem, there is a huge difference between the values of $\zeta_{f1}[t]$ $\zeta_{f2}[t]$ $\zeta_{f3}[t]$, that depend on $T^4(.)$, $T(.)$ and $G_s(t)s_{fs}(u_s(t))$. A fact that may cause numerical problems. To solve this problem, the matrix Φ is scaled by a diagonal matrix such that $Y = \Phi\Lambda\alpha_L$, with $\alpha_L = \Lambda^{-1}\alpha$.

The results of the off-line identification corresponding to a time window of fig. 3 are shown on fig. 4, where the sample temperature $T_s(t)$ (blue colour) and the one-step ahead prediction are very similar. The model output with the initial state set to $T_s[400]$ is shown in green colour. In both cases the model outputs are good approximations of the process dynamics.

The scaling matrix was selected as $diag(\Lambda) = [2.0 \times 10^{-11}, 1.0\times10^{-2}, 1.0\times10^{-1}]$, the estimates of $\bar{\alpha}_1$, $\bar{\alpha}_2$ and $\bar{\alpha}_3$ are respectively, 1.590×10^{-11}, 1.581×10^{-2}, 2.608×10^{-1}.

An important aspect that the model can provide is the quantification of the relation between the energy loss by radiation described by the term $\bar{\alpha}_1[T_s^4(t) - T_e^4(t)]$ that is nonlinear, and the term corresponding to energy loss by convection $\bar{\alpha}_2[T_s(t) - T_e(t)]$, that has a linear contribution to the temperature dynamics. The comparison is presented

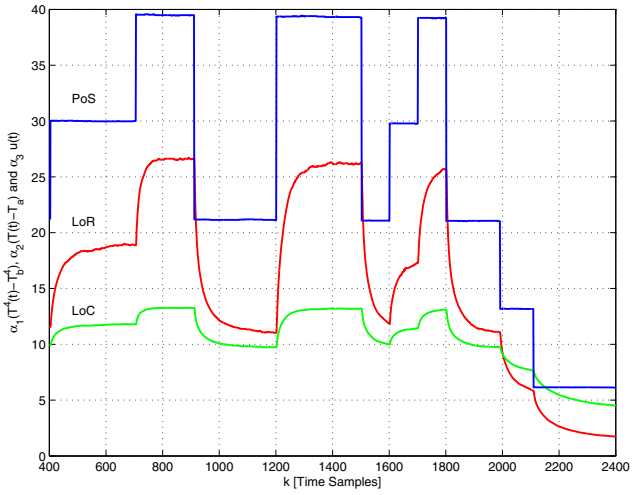

Fig. 5. Comparing the contribution of each term of temperature model dynamics. LoC - Loss by Convection, LoR - Loss by Radiation, PoS - Power absorption

on fig. 5, from which it can be concluded that the nonlinear term dominates for temperatures higher than $900K$. Below this temperature value the energy loss by convection have a bigger contribution to the temperature dynamics.

4. CONTROL LAW DESIGN

The control law is design based on the minimization of the cost function

$$J(N) = \sum_{j=1}^{N} [(T_s(k+j) - T_R(k+j))^2 + \rho(\Delta u(t+j-1))^2] \quad (13)$$

where N defines the control horizon corresponding to the time window $N * h$, with h being the sampling interval. $T_R(.)$ represents the future temperature profile, $T_s(.)$ represents the output of the process to be controlled, and $\rho > 0$ is an adjustable parameter that weights the future incremental control actions $\Delta u(.)$.

In order to compute the predictors that relate the process output $T_s(.)$ with the control increment $\Delta u(.)$ one considers the discrete time version of (2)

$$\begin{aligned} T_s(k+1) = T_s(k) - h\bar{\alpha}_1[T_s^4(k) - T_e^4(k)] \\ -h\bar{\alpha}_2[T_s(k) - T_e(k)] + h\bar{\alpha}_3 u(k)\,, \end{aligned} \quad (14)$$

where $u(k) = G_s(k)s_{fs}(u_s(k))$.

Considering now (14) at time k and computing $\Delta T_s(k+1) = T_s(k+1) - T_s(k)$, an incremental model of the process is obtained,

$$\begin{aligned} \Delta T_s(k+1) = \Delta T_s(k) - h\bar{\alpha}_1[T_s^4(k) - T_s^4(k-1)] \\ -h\bar{\alpha}_2\Delta T_s(k) + h\bar{\alpha}_3\Delta u(k)\,. \end{aligned} \quad (15)$$

where the nonlinear term $T_s^4(k) - T_s^4(k-1)$ can be approximated by a Taylor expansion

$$T_s^4(k) - T_s^4(k-1) \simeq 4T_s^3(k-1)\Delta T_s(k)\,.$$

Assuming that the tracking error is small, the term $T_s^3(k-1)$ can be replaced by the reference $T_R^3(k-1)$ and, the incremental model given by eq. (15) is written as

$$\Delta T_s(k+1) = \Phi(k+1,k)\Delta T_s(k) + \Gamma\Delta u(k)\,, \quad (16)$$

$$T_s(k+1) = T_s(k) + \Delta T_s(k+1) \quad (17)$$

where

$$\Phi(k+1,k) = 1 - h\bar{\alpha}_1 4T_R^3(k-1) - h\bar{\alpha}_2 \quad (18)$$

$$\Gamma = h\bar{\alpha}_3 \quad (19)$$

The output predictors from $k+1$ to $k+N$ can now be computed using eq.s (16) and (17).

$$\begin{aligned} \Delta T_s(k+1) &= \Phi(k+1,k)\Delta T_s(k) + \Gamma\Delta u(k) \\ \Delta T_s(k+2) &= \Phi(k+2,k+1)\Delta T_s(k+1) + \Gamma\Delta u(k+1) \\ \Delta T_s(k+3) &= \Phi(k+3,k+2)\Delta T_s(k+2) + \Gamma\Delta u(k+2) \\ &\ldots = \ldots \\ \Delta T_s(k+N) &= \Phi(k+N,k+N-1)\Delta T_s(k+N-1) + \\ &\quad +\Gamma\Delta u(k+N-1) \end{aligned}$$

$$\begin{aligned} T_s(k+1) &= T_s(k) + \Delta T_s(k+1) \\ T_s(k+2) &= T_s(k) + \Delta T_s(k+1) + \Delta T_s(k+2) \\ T_s(k+3) &= T_s(k) + \Delta T_s(k+1) + \Delta T_s(k+2) + \Delta T_s(k+3) \\ &\ldots = \ldots \\ T_s(k+N) &= T_s(k) + \Delta T_s(k+1) + \ldots + \Delta T_s(k+N) \end{aligned}$$

$$T_s(k+1) = T_s(k) + \Phi(k+1,k)\Delta T_s(k) + \Gamma\Delta u(k) \quad (20)$$

$$\begin{aligned} T_s(k+2) = T_s(k) + \Phi(k+1,k)\Delta T_s(k) + \Gamma\Delta u(k) \\ + \Phi(k+2,k+1)\Phi(k+1,k)\Delta T_s(k) \\ + \Phi(k+2,k+1)\Gamma\Delta u(k) + \Gamma\Delta u(k+1) \end{aligned} \quad (21)$$

$$T_s(k+3) = ... \quad (22)$$

Rearranging the terms, the predictors can be written in a matrix equation that has the following form,

$$T_p = I_{n,1}T_s(k) + S\Delta T_s(k) + W\Delta U\,, \quad (23)$$

where

$$T_p = [T_s(k+1)\ T_s(k+2)\ \ldots\ T_s(k+N)]'\,,$$
$$I_{(n,1)} = [1\ 1\ \ldots\ 1]$$

S is a column vector and W is a square matrix, and

$$\Delta U = [\Delta u(k)\ \Delta u(k+1)\ \ldots\ \Delta u(k+N-1)].$$

Using (23) in the cost function (13), and minimizing it with respect to the incremental control actions, the future incremental control actions are given by

$$\Delta U = -(W'W + \rho I)^{-1}W'[I_{n,1}T_s(k) - T_R + S\Delta Ts_(k)]\,. \quad (24)$$

In practice only the first value of ΔU, that is $\Delta u(k)$, is applied to the process.

The equations that define the control law are

$$\Delta u(k) = K_1(T(k) - T_R(k)) + K_2(T_s(k) - T_s(k-1))\,, \quad (25)$$

$$u(k) = u(k-1) + \Delta u(k) \quad (26)$$

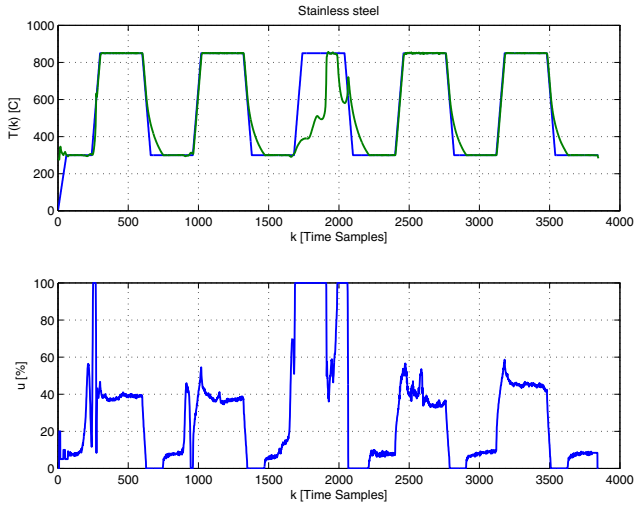

Fig. 6. Exp1: Temperature control of a stainless steel sample with the predictive controller with integral action. During this experiment the sun power has a low level and it is not stable.

and

$$u_s(k) = s_{fs}^{-1}(u(k)/G_s(k)) \tag{27}$$

that is used to compensate the static function of the shutter and the sun power variability. Note that, in order to simplify controller implementation, the controller gains are computed off-line and an anti-windup mechanism is used to readjust the control when it is saturated.

The robustness of the control algorithm can be analysed using the methodology described in Stoica et al. (2007).

5. PRACTICAL EVALUATION OF THE CONTROL LAW

The controller gains are computed off-line using $\bar{\alpha}_1$, $\bar{\alpha}_2$ and $\bar{\alpha}_3$. These parameters values are computed off-line from model identification using process data collected from a previous experiment.

To simplify the implementation of the controller, the gains are kept constant, independent of the temperature reference changes. Thus the terms of $\phi(.,.)$ use a constant (the same) value for the T_R^3 term, usually an higher value of the reference temperature signal that ensures a good model description when the process is operating near the sample temperature melting point.

Figure 6 shows the results obtained during an experiment using the predictive controller with integral action to control the temperature of a stainless steel sample. The controller gains are $K_1 = 1.0585$ and $K_2 = -3.282$ that are obtained for $\rho = 0.5$ and $N = 25$. During this experiment the sun power has a low level, that is shown on figure 7 and was not constant. This fact causes perturbations on the temperature of the sample that the controller is able to compensate in part, since the sun available power was not enough to heat the sample to the temperature reference.

The effect of the control weight ρ was evaluated for four different values, $\rho_1 = 0.001$ ($K_1 = 6.7223$, $K_2 = -7.0317$), $\rho_2 = 0.01$ ($K_1 = 4.3458$, $K_2 = -5.937$), $\rho_3 = 0.1$ ($K_1 =$

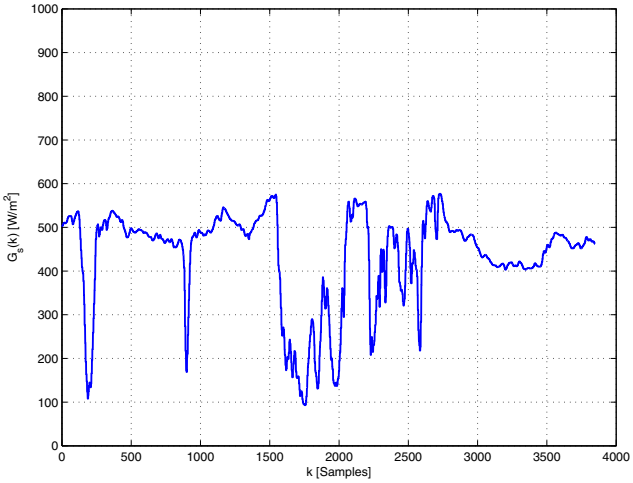

Fig. 7. Exp1: Sun power variability that was present during experiment 1, corresponding to the results shown in fig.(6). These conditions are usually not used to perform temperature stress tests.

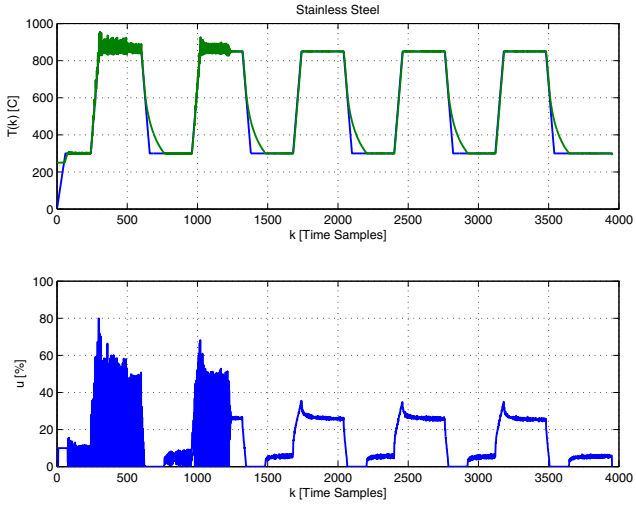

Fig. 8. Exp2: Evaluation of the control weight ρ on the temperature control, ρ_1 was used at $k = 0$, ρ_2 at $k = 500$, ρ_3 at $k = 1300$ and ρ_4 was used at $k = 3100$. During this experiment the sun power almost constant near $875W/m^2$. By increasing the control weight, the control signal is smoother and the controller has a better performance.

2.02321, $K_2 = -4.3504$) and $\rho_3 = 0.2$ ($K_1 = 1.5433$, $K_2 = -3.8565$). The corresponding controller gains were used during the experiment at the following time samples: ρ_1 was used at $k = 0$, ρ_2 at $k = 500$, ρ_3 at $k = 1300$, and ρ_4 was used at $k = 3100$. The results are shown in the fig. 8, low values on the control weight generate high gain values causing noise amplification on the control signal and degrades the performance. This experiment also shows that switching control can also be employed to selected adequate gains from a set of gains computed off-line.

From the previous experiment it can be concluded that a good temperature tracking is obtained during the increase of the temperature reference signal and during the time intervals where the reference signal is constant. During the

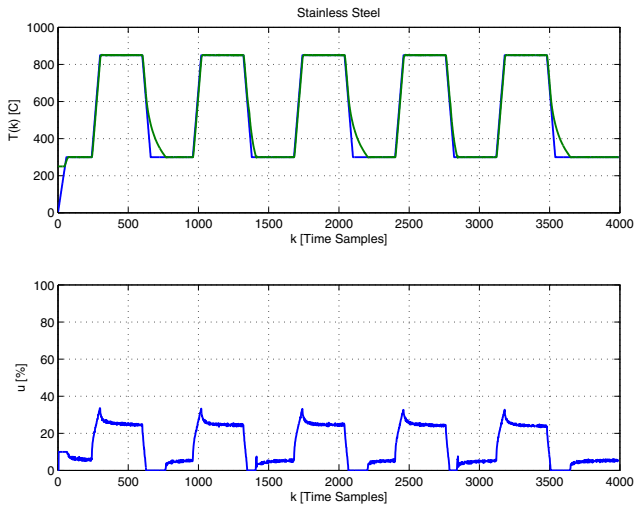

Fig. 9. Exp3: Using active cooling, application of air flow, to improve the temperature tracking during the second and fourth reference cycles (reference decrease).

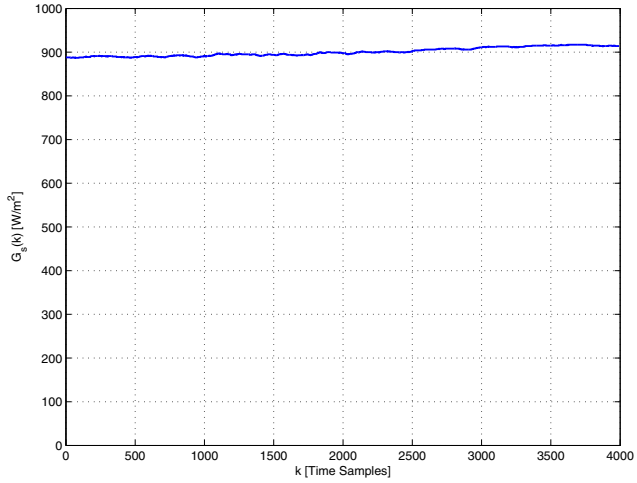

Fig. 10. Exp3: Sun power during experiment 3 corresponding to the results shown in fig.(9), that represent good conditions for temperature stress tests.

decrease of the temperature reference, the natural energy loss by radiation and by convection do not allow a good tracking, since the rate of energy loss is not adequate. To tackle this situation active cooling (air flow) is employed to decrease the temperature of the sample. The air flow is applied when the control signal of the shutter is zero, the shutter is closed, and the sample temperature is above the reference. This action can be considered as a disturbance that the controller must compensate when the temperature of the sample becomes lower than the temperature reference. The results of this experiment are shown in fig. 9. The application of the air flow occurs during the second and fourth reference cycles (reference decrease). During this experiment the solar power was almost constant as shown in the fig. 10.

6. CONCLUSION

This paper describes the design of a control system for solar furnaces for temperature cycling stress tests. The process dynamics that accounts for the contribution of losses by radiation and by convection and solar energy absorption is characterized using off-line model identification.

The control methodology, MPC with integral action, explores the structure of the process nonlinear dynamics, where the controller gains are computed off-line. This methodology avoids the use of online adaptation mechanisms that may cause stability problems during stress test. Experiment test results show that the proposed methodology has a good performance and can be used with active cooling to improve the temperature tracking during the decrease of the temperature profile. It is also demonstrated that switching control can be employed to selected adequate gains from a set of gains computed off-line.

ACKNOWLEDGEMENTS

This research has been supported by the European projet SFERA-2 and the program UID/CEC/50021/2013, and PROMES that provide the conditions, materials and equipment, without them the experimental tests were not possible.

REFERENCES

Berenguel, M., Camacho, E., Garcia-Martin, F., and Rubio, F. (1999). Temperature control of a solar furnace. *IEEE Control Systems*, 19(1), 8–24.

Clarke, D.W., Mohtadi, C., and Tuffs, P.S. (1987). Generalized predictive control—part i. the basic algorithm. *Automatica*, 23(2), 137–148.

Costa, B.A. and Lemos, J. (2009). Singular perturbation stability conditions for adaptive control of a solar furnace with actuator dynamics. *European Control Conference 2009 Budapest Hungary*.

Costa, B.A. and Lemos, J. (2012). Predictive adaptive temperature control in a solar furnace for material stress tests. *IEEE Multi-conference on Systems and Control 2012 Dubrovnik Croatia*.

Costa, B.A. and Lemos, J. (2014a). Temperature control of a solar furnace with exact linearization and off-line identification. *CONTROLO2014 Proceedings of the 11th Portuguese Conference on Automatic Control*, 321, 321–330.

Costa, B.A. and Lemos, J. (2016). Control of a solar furnance using active cooling. *European Control Conference 2016 Aalborg, Denmark*.

Costa, B.A. and Lemos, J.M. (2014b). Optimal control of the temperature in a solar furnace. *Optimal Control Applications and Methods*.

Stoica, C., Rodriguez-Ayerbe, P., and Dumur, D. (2007). Off-line robustness improvement of predictive control laws in state-space description. In *Control Automation, 2007. MED '07. Mediterranean Conference on*, 1–6.